# Metal Oleate Induced Etching and Growth of Semiconductor Nanocrystals, Nanorods, and Their Heterostructures

Nuri Oh and Moonsub Shim*

Department of Materials Science and Engineering, University of Illinois at Urbana—Champaign, Urbana, Illinois 61801, United States

S *Supporting Information*

ABSTRACT: Unexpected etching of nanocrystals, nanorods, and their hetero-structures by one of the most commonly used metal precursors, metal oleates, is reported. Zn oleate is shown to etch CdS nanorods anisotropically, where the length decreases without a significant change in the diameter. Sodium oleate enhances the etch rate, whereas oleic acid alone does not cause etching, indicating the importance of the countercation on the rate of oleate induced etching. Subsequent addition of Se precursors to the partially etched nanorods in Zn oleate solution can lead to epitaxial growth of CdSe particles rather than the expected ZnSe growth, despite an excess amount of Zn precursors being present. The composition of this epitaxial growth can be varied from CdSe to ZnSe, depending on the amount of excess oleic acid or the reaction temperature. Similar tuning of composition can be observed when starting with collinear CdSe/CdS/CdSe rod/rod/rod heterostructures and spherical CdS (or CdSe/CdS core/shell) nanocryst-

als. Conversion of collinear rod/rod/rod structures to barbells and interesting rod growth from nearly spherical particles among other structures can also result due to the initial etching effect of metal oleates. These observations have important implications on our understanding of nanocrystal heterostructure synthesis and open up new routes to varying the composition and morphology of these materials.
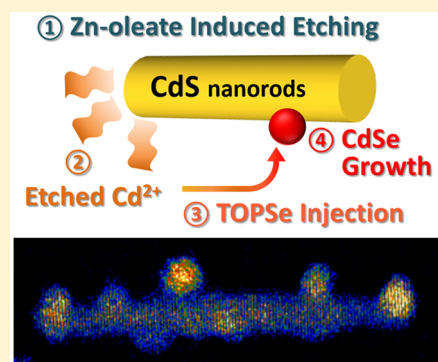
INTRODUCTION

Advances in chemical synthesis of semiconductor nanocrystals (NCs) have led to an exquisite control over the size, size distribution, composition, and even shape of a variety of materials into colloidal format that provides versatility in processing.[1−5] Metal complexes with long chain carboxylates,[6−10] amines,[10−14] and phosphonates[15−18] are some of the most commonly used precursors for the synthesis of a variety of NCs. Such metal precursors are also important for the growth of heterostructures that provide enhanced optical/electronic properties[19,20] often necessary for a successful implementation of new or improved applications utilizing these materials. For example, type I straddling band offset core/shell structures allow high photoluminescence (PL) necessary for biomedical imaging,[21−23] and type II staggered band offset heterostructures provide efficient photoinduced charge separation useful for photocatalysis or photovoltaics.[24−27] Synthetic approaches to achieve well-defined and controlled NC heterostructures usually require exposure of presynthesized NCs to metal complex precursors at elevated temperatures for an extended period of time. An extreme example is the SILAR method to grow a thick CdS shell on CdSe NCs, which would take more than 5 days at 240 °C for 19 CdS layers.[28] Carboxylic acids and related coordinating molecules (often in conjunction with another reagent) are known to etch and digest metal oxides.[29,30] In fact, such an approach is commonly used to make metal oxide powders soluble in organic solvents

to be used for NC synthesis.[31,32] Yet, very little attention has been given to such etching effects during the synthesis of semiconductor NCs, especially in growing heterostructures. Here, we show surprising anisotropic etching of CdS nanorods (NRs) and CdS/CdSe nanorod heterostructures (NRHs) by one of the most commonly used reagents, metal oleates. It is the presence of metal oleates rather than oleic acid that leads to this unexpected etching. Addition of a more reactive chalcogen source can lead to growth that uses the etched metal ions in solution, and the morphology and the composition of the resulting heterostructures can be varied by the amount of excess oleic acid and the reaction temperature. We also demonstrate that similar etching and growth effects can be seen in spherical NCs, including core/shell structures, leading to an interesting growth of islands or NRs from spherical NCs without the need for surface capping molecules that facilitate rod/directional growth.

RESULTS AND DISCUSSION

While etching of various NCs, induced or assisted by amines,[33−35] various oxidants,[36−39] or photochemical means,[40−42] as well as anisotropic etching[43] by certain acids[44] or bases,[45] has been observed, metal carboxylates used as actual cation sources for NC growth causing such an effect have not
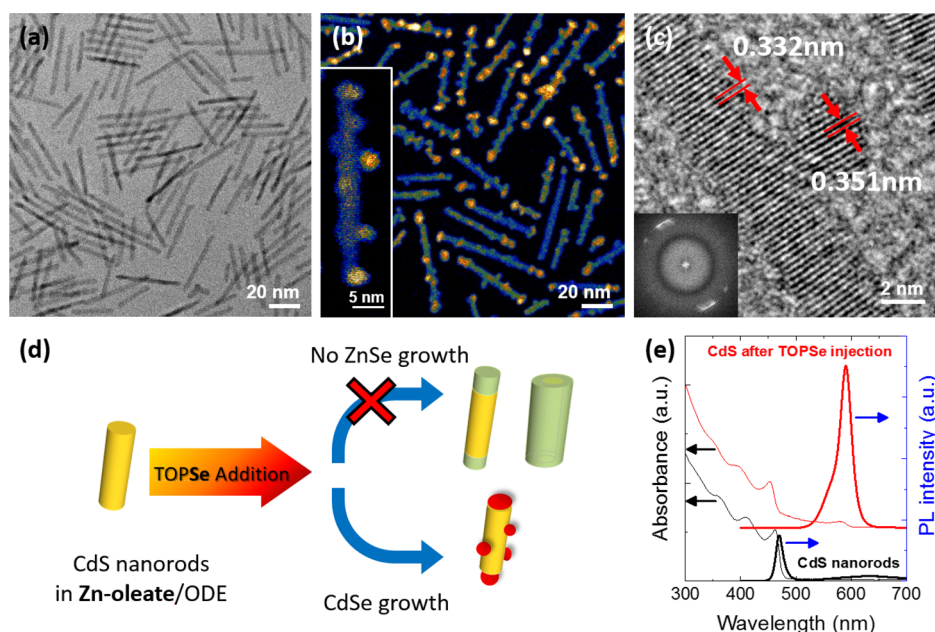
Figure 1. Shape evolution of CdS nanorods in Zn oleate/ODE solution before and after TOPSe injection. (a) TEM image of CdS nanorod seeds. (b) High-resolution Z-contrast STEM image after injecting TOPSe. Brighter spots shown at the tips and the dots on the sides of nanorods indicate heavier elements, corresponding to CdSe. (c) Magnified TEM image of side growth of a secondary component on CdS nanorods. The lattice parameter of the secondary component is larger than that of the CdS nanorods and consistent with CdSe. (d) Schematic illustration of multiple CdSe growth on CdS nanorods due to unexpected etching rather than initially intended ZnSe growth. (e) Absorption and emission spectra of CdS nanorods before and after TOPSe injection.

been reported. This etching effect may have been concealed because it is difficult to distinguish the subtle size change before and after the reaction in spherical NCs.

We became aware of this etching when we attempted to grow ZnSe on CdS NRs. When CdS NRs, after several purification steps to remove leftover Cd and S reagents, were added to Zn oleate solution in octadecene (ODE), the subsequent injection of trioctylphosphine selenide (TOPSe) led to the growth of islands of CdSe rather than the anticipated ZnSe on the seed CdS NRs. Figure 1 shows transmission electron microscopy (TEM) images and absorption/PL spectra of the CdS NRs before and after this etch/growth process. Injection of TOPSe into CdS NR/Zn oleate solution leads to an absorption peak at ~580 nm and a PL maximum at ~590 nm, expected of CdSe NC band edge transitions, while the strong CdS absorption peak at 450 nm remains. Much higher Z-contrast intensity in the scanning transmission electron microscopy (STEM) image and the larger lattice spacing measured in the high-resolution TEM image in Figures 1b and c, respectively, confirm that the epitaxially grown particles on the sides and tips of CdS NRs do indeed correspond to CdSe rather than ZnSe (Zn is lighter than Cd, and ZnSe should have smaller lattice spacing than CdS; Supporting Information Table S1).[46] High-resolution aberration-corrected STEM images (Supporting Information Figure S1) further verify that the Z-contrast between cation and anion columns is consistent with CdSe growth. Energy dispersive X-ray spectroscopy (EDS) analysis also indicates that there is little or no increase in Zn content upon TOPSe addition compared to NRs exposed only to Zn oleate solution (Supporting Information Table S2). Additional TEM images and diffraction are shown in Supporting Information Figure S2. Based on these results, we conclude that particles of wurtzite CdSe form on the sides and tips of CdS NRs without any additional Cd precursors and

despite the excess amount of Zn precursors in the reaction mixture.

In this unexpected growth of CdSe on CdS NRs during an attempt to grow ZnSe, the only significant source of Cd is the CdS NRs themselves, implying possible etching of CdS NRs. To examine this potential etching effect and, if it is indeed occurring, to identify the etchant, purified CdS NRs were first exposed to an ODE solution containing only oleic acid and examined at different times of heating. Figure 2a shows a TEM image of CdS NRs exposed to oleic acid in ODE at 250 °C for 2 h. The corresponding TEM image of CdS NRs before this treatment is shown in Figure 1a. No obvious structural changes are observable. When the same treatment was carried out using Zn oleate instead of oleic acid, a noticeable decrease in length without a significant change in diameter was seen, as shown in Figure 2b. This anisotropic etching may be due to different surface energies of different facets and/or expected lower ligand coverage at the high-curvature tips. The use of Na oleate caused an even more noticeable decrease in length with a slight increase in diameter, indicating a much faster etch rate with possible partial regrowth or ripening from free Cd/S in solution (Figure 2c). For these three reaction conditions, the same initial CdS NR solution was purified and divided into three batches. We note that when Zn oleate was synthesized by ZnO instead of Zn acetate or when higher purity (99%) oleic acid was used, the results were the same as the Zn oleate case in Figure 2 (Supporting Information Figures S3 and S4). We also rule out the potential role of residual water (21 ppm as measured by Karl Fischer titration) because (1) the amount water is at least an order of magnitude smaller than the expected amount of Cd being etched out and (2) despite the fact that the same amount of trace water was measured in both Zn oleate and oleic acid cases, the latter case did not lead to etching. Therefore, we conclude that impurities and byproducts
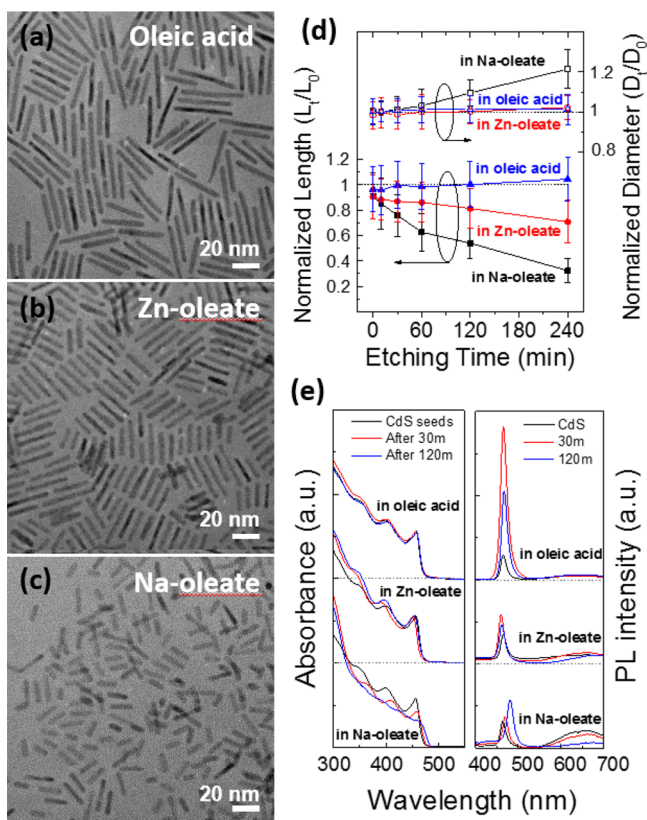
Figure 2. Etching effects of metal oleates on CdS nanorods. TEM image of CdS nanorod seeds in (a) oleic acid, (b) Zn oleate, and (c) Na oleate/ODE solution for 4 h at 250 °C, respectively. (d) Average length and diameter changes in each solution. CdS nanorods in Na oleate solution become much shorter and more ripened than in Zn oleate solution. There is no significant change in oleic acid solution. (e) Absorption and emission spectra before and after etching in each solution at 250 °C for 30 min and 2 h, as indicated.

do not have a significant effect or are evaporated off (e.g., acetate from Zn acetate being lost as acetic acid).

Figure 2d compares the changes in length and diameter of CdS NRs with annealing time using these three different reagents, quantifying the qualitative TEM observations of Figures 2a, b, and c. The etching time 0 min in Figure 2d corresponds to the time when the CdS NR solution reaches 250 °C (heat up time of 10 min). Figure 2e compares the absorption and PL spectra before and after 30 min and 2 h exposure to oleic acid or metal oleate solution. As expected, no significant changes are seen in the absorption spectra of oleic acid and Zn oleate treated CdS NRs, since the diameter of the NRs is not significantly altered in both cases. Oleic acid does, however, appear to improve surface properties, as suggested by the increase in the CdS NR band edge PL. Na oleate treatment, on the other hand, causes significant redshift and broadening of the CdS NR absorption features, consistent with increasing diameter and decreasing aspect ratio observed in the TEM images. Furthermore, Fourier transform infrared spectroscopy of CdS NR films prepared before and after Zn oleate solution exposure shows that the majority of the surface ligands change from phosphonic acid to oleate whereas treatment with only oleic acid leads to phosphonic acid remaining on CdS NRs (Supporting Figure S5).[47,48] That is, (metal) oleates can cause surface ligand replacement but oleic acid alone cannot. These observations together indicate that it is the oleate anion rather

than oleic acid that causes the etching of the NRs and the strength of coordination to the countercation dictates the reactivity and therefore the etch rate. We note that there is a very recent report of oleate etching of rare-earth-doped fluoride NCs,[45] further emphasizing the importance of this unexpected etching.

To provide some insights on a possible mechanism of etching, we consider the following. In addition to the importance of the presence of oleate anions, the EDS results shown in Supporting Information Table S2 indicate about 5% Zn being present in CdS NRs after exposure to Zn oleate solution. We then expect Zn to be adsorbed on the surface of CdS NRs. In addition, it is well-known that sulfur can be easily dissolved in ODE, especially at elevated temperatures and sulfur anions may form metal complexes or be lost as H_2S.[49,50] Based on these observations, we suggest the following reaction (unbalanced) for Zn oleate induced etching of CdS NRs.

$$(CdS)_{ligand} + Zn^{2+}(Ol^-)_2$$
$$\rightarrow Cd^{2+}(Ol^-)_2 + S_x^{n-} + (Zn^{2+})_{ligand} + (Zn^{2+})_{adsorbed}$$
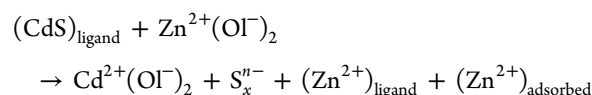
Here, $(CdS)_{ligand}$ corresponds to Cd and S on the surface of ligand passivated CdS NRs, Ol^- refers to oleate anion, S_x^{n-} is sulfur dissolved in ODE solution or sulfide (possibly as metal polysulfide complexes in solution or lost as H_2S gas),[49−51] $(Zn^{2+})_{ligand}$ is Zn complex in solution coordinated by ligands, and $(Zn^{2+})_{adsorbed}$ is Zn species adsorbed on the surface of NRs. That is, Zn^{2+} in solution and Cd^{2+} on the surface of CdS NRs exchange coordinating molecules, leading to Cd oleate complex and solvated S/S^{2-} in solution. Resulting Zn^{2+} can be either adsorbed on the NR surface or remain in solution by being coordinated to the surface ligands that may have come off the NRs.

The above-discussed etching effects are further verified by the products arising from the addition of TOPSe to CdS NRs that have been etched. When CdS NRs are treated with oleic acid, we do not observe a secondary component growth with Se precursor addition, as expected since there is an insignificant amount of etched Cd. This observation also verifies that unreacted Cd precursors from the initial CdS NR synthesis have been sufficiently removed. Na or Zn oleate treated CdS NRs, on the other hand, exhibit a significant growth of the second component upon Se precursor addition. Side and tip growths of CdSe dots result from Zn oleate etching and added TOPSe as seen in Figure 1 and Supporting Information Figures S2, S3, and S4 and as discussed above. In the case of Na oleate etching, a significant amount of separate homogeneous nucleation of CdSe NCs occurs, presumably due to a relatively high concentration of reactive Cd in solution (Supporting Information Figure S6). The observed side growth of CdSe on CdS NRs with nearly spherical shape and large contact angle in the Zn oleate case is uncommon compared to the more expected growth along the rod axis (or shell growth) for NRHs. Hence, metal oleate induced etching can play an important role not only in the synthesis of semiconductor NCs but also in the synthesis of their heterostructures, in particular, in altering the morphology and composition of the products.

Along with the unexpected etching effect of metal oleates, the presence of excess oleic acid and the reaction temperature can provide some control over the composition of resulting NRHs, which can in turn alter the morphology. Although many reported syntheses of NCs vary in the ratio of oleic acid to metal salts used and therefore the amount of excess oleic acid
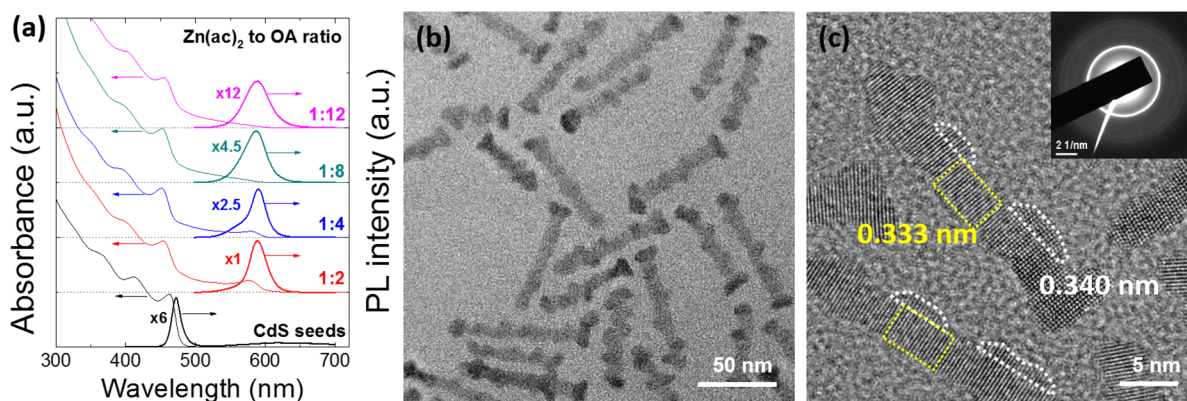
Figure 3. Effect of excess oleic acid on metal oleate induced etching and subsequent growth. (a) Absorption and emission spectra of NRHs arising from Zn oleate etching of CdS NRs with different amounts of excess oleic acid followed by TOPSe injection. (b) Low- and (c) high-magnification TEM images of the NRHs resulting from using a 1:12 ratio of Zn acetate and oleic acid in ODE solution. The center part of the NRHs shows the similar lattice spacing with (002) planes of wurtzite CdS, while the components grown at the side faces has smaller lattice spacing than the (002) planes of wurtzite CdSe.
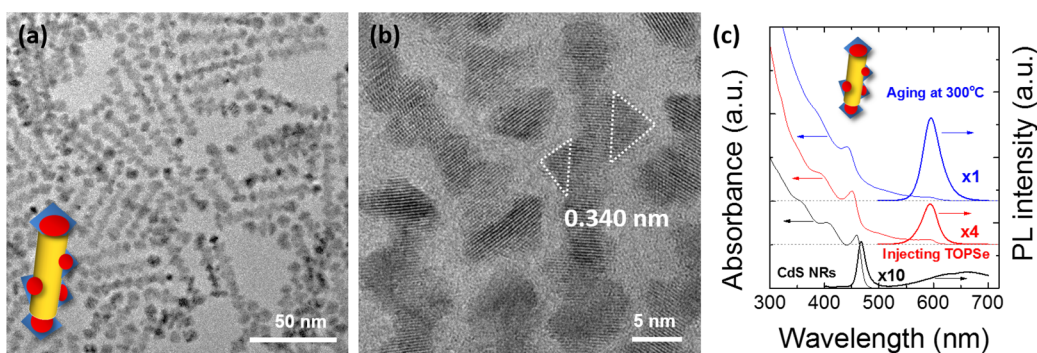

Figure 4. Effect of reaction temperature on Zn content in the second phase growth. (a) Low- and (b) high-magnification TEM images of the NRHs annealed at 300 °C. The pyramidal shaped second phase growth has smaller lattice spacing than the (002) planes of wurtzite CdSe. (c) Absorption and emission spectra of the resulting NRHs after injecting TOPSe following by annealing at 300 °C for 2 min.

present in the reaction mixture,[7,45,52] little consideration has been given to how this varying amount of excess oleic acid affects the growth of NCs or their heterostructures. Yet, whether or not excess oleic acid is present can alter products profoundly. For example, a CdS shell can be grown on CdSe NCs using Cd oleate if there is an excess amount of oleic acid, but the same growth conditions without excess oleic acid have been shown to lead to separate nucleation of CdS particles.[52] Excess carboxylic acid has also been suggested to increase the solubility of metal precursors and thus suppress their reactivity.[53] Similar effects of excess oleic acid can be seen in our system of CdS-based NRHs and can be exploited to alter the composition and morphology of the resulting NRHs. Without excess oleic acid, separate CdSe particles can nucleate upon TOPSe addition for the Na oleate case where there is a large degree of etching and, therefore, a high concentration of Cd source in solution, similar to the previous unsuccessful CdS shell growth attempt on CdSe NCs without excess oleic acid.[52] When Zn oleate is used where milder etching conditions lead to a lower concentration of Cd source in solution, CdSe particles of nearly spherical shape grow on both the tips and the sides of CdS NRs with large contact angles. This type of growth was observed when using Zn oleate prepared by a 1:2 or 1:4 molar ratio of Zn acetate:oleic acid with no additional oleic acid added to the reaction mixture. On the other hand, Figure 3 shows that, after etching of CdS NRs with Zn oleate prepared with excess oleic acid (1:12 molar ratio of Zn acetate:oleic acid), the

addition of TOPSe leads to tip and side growth of particles that have smaller lattice spacing and with significantly smaller contact angles. The smaller lattice spacing, smaller contact angle, and hence larger interface areas with CdS may be explained by the formation of CdZnSe alloy particles, which would better match the CdS lattice than CdSe would (Supporting Information Table S1). The absorption and PL spectra are also distinct from CdSe growth in the absence of excess oleic acid. The distinct CdSe band edge absorption peak converts to an absorption tail in the red as the amount of excess oleic acid in the reaction mixture is increased (Figure 3a). The PL intensity normalized to absorption at the excitation wavelength decreases by about an order of magnitude and becomes broader in width with increasing oleic acid amount. The full-width-at-half-maximum of the PL peak increases from 26.5 nm (95 meV) to 41.5 nm (149 meV) from the no excess oleic acid case to the largest amount of excess oleic acid examined here (bottom-most and topmost spectra of Figure 3a, respectively). The increased line width and the drastic decrease in intensity of PL for the largest oleic acid amount case are consistent with spectral features arising from type II band offset between CdS and ZnSe (or Zn-rich CdZnSe). EDS results also show that a significantly larger amount of Zn gets incorporated during the second component growth on CdS NRs with excess oleic acid (Zn: 29.9 at. % ± 0.4, Supporting Information Table S3) than without (Zn: 8.1 at. % ± 0.4, Supporting Information Table S2). This enhanced incorporation of Zn may be due to a
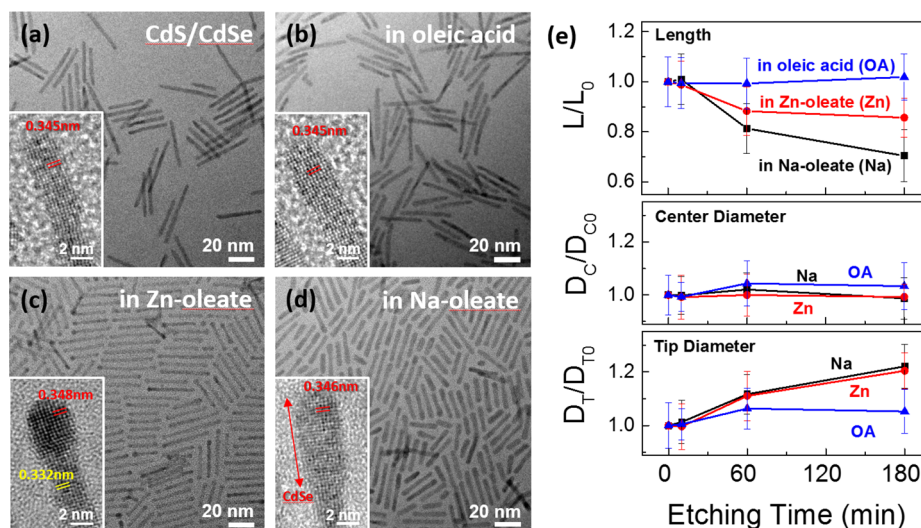
Figure 5. Effect of Zn oleate etching on CdSe/CdS/CdSe rod−rod−rod shaped NRHs. TEM images of (a) CdSe/CdS/CdSe seeds, after etching by (b) oleic acid (no etching), (c) Zn oleate, and (d) Na oleate for 3 h at 250 °C. (e) Length and tip/center diameter changes in different oleate/ODE solutions.
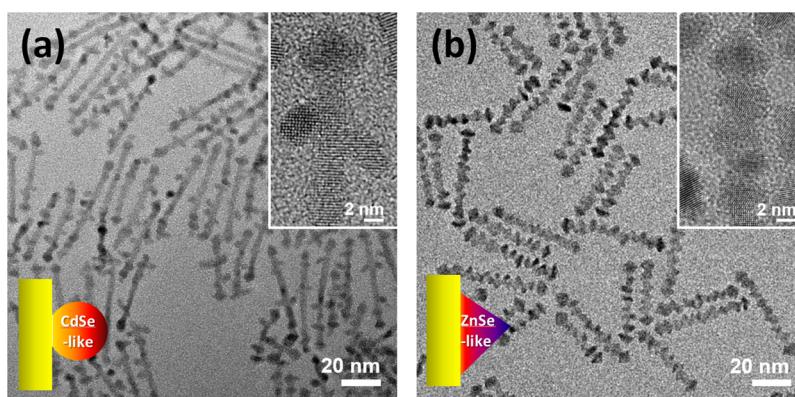
Figure 6. Effect of excess oleic acid on CdSe/CdS/CdSe NRHs with TOPSe injection. TEM images of (a) the resulting NRHs after etching by Zn oleate without excess oleic acid followed by injecting TOPSe and (b) the resulting NRHs with excess oleic acid.

better stabilization of etched Cd in solution by excess oleic acid, effectively reducing its reactivity,[53] and therefore, Zn oleate becomes competitive in reacting with added TOPSe.

Another approach to increasing Zn content during the second phase growth step is to increase the reaction temperature. After CdSe growth on CdS NRs via Zn oleate etching without excess oleic acid, if the reaction temperature is increased to 300 °C, the initial near spherical CdSe particles on the sides and tips of CdS NRs (Figure 1) become larger and change to triangular cross-section, as shown in Figure 4. There is a significant decrease in the lattice constant of the particles grown on the sides of the NRs from 0.353 nm of CdSe at 250 °C (Figure 1c) to 0.340 nm after growth at 300 °C (Figure 4b). The UV/vis spectrum in Figure 4c shows a slight red-shift of the band edge absorption near 580 nm as well as an increasing UV absorption. The PL efficiency increases significantly (∼30% maximum PL efficiency observed) without much increase in the line width. These observations, combined with the EDS results in Supporting Information Table S2 show a significant increase in Zn content (from 8.1 at. % to 24.7 at. %) only after annealing at 300 °C, are consistent with CdSe growth at 250 °C being maintained (or slightly increasing in size) along with ZnSe- or Zn-rich CdZnSe alloy overgrowth upon heating to 300 °C.

Hence, the reaction temperature and the amount of excess oleic acid present are critical parameters that can dictate whether type II staggered band offset (e.g., CdS/ZnSe) or type I straddling band offset (e.g., CdS/CdSe) heterostructures are obtained.

With a better understanding of how metal oleates alter the structure of CdS NRs and the subsequent heterostructure formation step, we now discuss how other CdS-containing NC and NR heterostructures are affected by this etching effect. Figure 5 summarizes the key results of oleic acid, Zn oleate, and Na oleate treatments of presynthesized and cleaned CdSe/CdS/CdSe collinear rod/rod/rod NRHs (referred to as CdS/CdSe NRHs from here on). Similar to the CdS NR case, no significant changes are observed with oleic acid, and decreasing lengths without a significant change in diameter (at the center of the NRs) are seen for Zn and Na oleate cases. The corresponding absorption and PL spectral changes are shown in Supporting Information Figure S7. The key difference is the ripening at the tips for the Zn and Na oleate cases, leading to barbell-like structures with Zn oleate resulting in more uniform tips. High-resolution TEM images in the insets of Figures 5c and 5d indicate that the ripened tips have lattice spacing consistent with CdSe, suggesting that it is mainly CdSe that

gets etched and that the higher reactivity of Se with Cd leads to regrowth or ripening. The addition of TOPSe to these CdS/CdSe NRHs etched/ripened by Zn oleate leads to similar growth, as seen in the CdS NR case, as shown in Figure 6. That is, without excess oleic acid, more CdSe-like particles with circular cross-section grow on the tips and sides of the initial NRHs whereas Zn-rich CdZnSe alloy particles with triangular cross-section appear with excess oleic acid.

It is interesting to note that CdS/CdSe NRHs originally exhibited two peaks in the PL, which begin to converge into a single peak upon this etching/ripening process (Figure 7). We
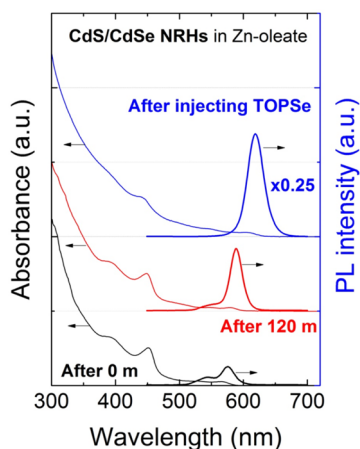
Figure 7. Absorption and emission spectra of CdS/CdSe NRHs before and after etching by Zn oleate at 250 °C for 2 h and after injecting TOPSe.

had previously shown that the two-peak PL arises from different sizes of CdSe at the tips from the initial single-pot synthesis of CdS/CdSe NRHs.[54] Upon etching/ripening due to Zn oleate, the asymmetric CdSe tips become similar in size, eventually leading to a single-peak PL. This ripening effect is also responsible for the change from a double-peak PL of CdS/CdSe NRHs to a single-peak PL upon ZnSe growth to form CdS/CdSe/ZnSe double heterojunction NRs (DHNRs).[54,55] We also note that the addition of TOPSe to CdS/CdSe NRHs in Zn oleate solution under the same conditions as in Figure 5c leads to a large degree of side growth (of mainly CdSe in the case of no excess oleic acid—Figure 6a) whereas TOPSe injection in the DHNR synthesis leads to mainly ZnSe shell

growth on CdSe tips. The key differences between these two syntheses are the temperature at which TOPSe is added and how the reaction temperature is changed after the addition. In the case of NRHs of Figures 5c and 6a, TOPSe is added at 250 °C after significant etching/ripening of the CdSe tips and allowed to react/grow at 250 °C. In the case of DHNRs, TOPSe is added at a lower temperature (i.e., 150 °C) where etching/ripening due to Zn oleate has not yet initiated and the reaction temperature is ramped up to 300 °C rapidly, favoring ZnSe growth, as expected from the results of increased reaction temperature discussed above (Supporting Information Figure S8).

The Zn oleate induced etching effects are also evident in the CdSe/CdS core/shell NC heterostructures upon addition of TOPSe. Although there may appear to be some faceting, when CdSe/CdS core/shell NCs are exposed to Zn oleate solution in ODE at 250 °C, the etching effects are not obvious in TEM images (Figures 8a and 8b). However, when TOPSe is added to the reaction mixture, surprisingly, CdSe rods begin to grow from nearly spherical dots in many instances (Figure 8c). Here, there are no capping molecules such as alkylphosphonic acids that induce preferential growth along a certain crystallographic direction. While further studies are necessary to sort out the mechanism that seems to prefer single rod growth on each dot, partial exposure of CdSe due to etching or limited concentration of reactive Cd in solution may be contributing to such a selective growth. Similar irregular shell and rod growths are also observed with and without excess oleic acid, respectively, when starting with CdS NCs rather than CdSe/CdS core/shell NCs (Supporting Information Figure S9). The addition of excess oleic acid with Zn oleate leads to irregular shell growth (Supporting Information Figure S9c), consistent with what may be expected based on growth of ZnSe or Zn-rich CdZnSe alloy particles with triangular cross-sections observed in the CdS NRs and CdS/CdSe NRHs.

CONCLUSION

We have shown that CdSe rather than intended ZnSe can grow on CdS NRs and NCs in Zn oleate solution despite the absence of intentionally added Cd precursors and an excess amount of Zn precursors. This surprising result arises from anisotropic etching of CdS by Zn oleate that leads to reactive Cd ions in solution. The degree of etching or the etch rate appears to depend on the strength of oleate coordination to its countercation. The composition and the morphology of the
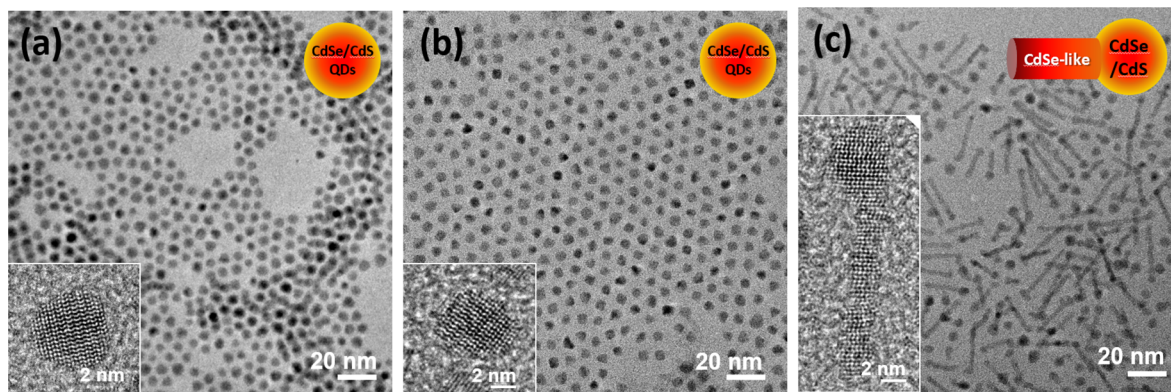
Figure 8. Effect of Zn oleate etching on CdSe/CdS core/shell NCs. TEM images of (a) CdSe/CdS core/shell seeds, (b) after etching with Zn oleate without excess oleic acid and (c) after injecting TOPSe into the solution of (b) at 250 °C.

second phase epitaxially grown on CdS NRs upon TOPSe addition after Zn oleate induced etching can be varied either by the amount of excess oleic acid present or by the reaction temperature. Excess oleic acid as well as higher temperature enhances Zn incorporation during the epitaxial growth, leading to more ZnSe-like structures with triangular cross-sections on CdS NRs. We have also shown that these effects are present in CdS/CdSe NRHs and CdSe/CdS core/shell NCs. In the case of CdS/CdSe NRHs which start out with asymmetric CdSe tips, etching and ripening of the tips lead to nearly symmetric barbell structures. For spherical NCs, conditions that favor CdSe growth lead to rod growth on the seed NCs whereas conditions that favor ZnSe growth lead to patchy shells. These findings not only imply how metal oleate induced etching can completely alter the composition of the products in the synthesis of NC and NR heterostructures but also may pave the path to novel heterostructures with complex shapes that may otherwise be difficult to achieve.

■ EXPERIMENTAL SECTION

Materials. Trioctylphosphine oxide (TOPO) (90%), trioctylphosphine (TOP) (90%), oleic acid (90%), oleylamine (OAm) (70%), octadecene (ODE) (90%), CdO (99.5%), CdCl$_2$, zinc acetate (99.99%), sulfur (99.998%), and selenium (99.99%) were obtained from Sigma-Aldrich. Sodium oleate (Na oleate) (>97%) was obtained from Tokyo Chemical Industry. N-Octadecylphosphonic acid (ODPA) was obtained from PCI Synthesis. ACS grade chloroform and methanol were obtained from Fischer Scientific. All chemicals were used as received.

Synthesis of CdS Nanorod Seeds. CdS NRs were prepared in a manner similar to established methods.[54] First, 2.0 g of TOPO, 0.67 g of ODPA and 0.128 g of CdO in a 50 mL three-neck round-bottom flask were degassed at 150 °C for 30 min under vacuum and then heated to 370 °C under Ar. After Cd-ODPA complex was formed at 370 °C, 32 mg of S dissolved in 2.0 mL of TOP was swiftly added into the flask with a syringe. Consequently, the reaction mixture was quenched to 330 °C where the CdS growth was carried out. After 15 min, CdS NR growth was terminated by cooling to room temperature. The final solution was dissolved in chloroform, centrifuged at 2000 rpm. The precipitate was redissolved in chloroform, and then prepared as a solution for the next step. This solution of CdS NRs had an optical density of 0.1 (for 1 cm optical path length) at the CdS band edge absorption peak when diluted by a factor of 100.

Synthesis of CdS/CdSe NRH Seeds. The synthesis of CdS/CdSe NRHs was carried out in a similar manner to an established method.[54,55] Following the formation of CdS NRs and cooling the reaction mixture from 330 to 250 °C, 20 mg of Se dissolved in 1.0 mL of TOP was slowly added at 250 °C at a rate of 4 mL/h via syringe pump (total injection time ~15 min). The reaction mixture was then allowed to stir for an additional 5 min at 250 °C before being rapidly cooled to room temperature. The final solution was dissolved in chloroform, and centrifuged at 2000 rpm. The precipitate was redissolved in chloroform, and then prepared as a solution for the next step. This solution of CdS/CdSe NRHs had an optical density of 0.1 (for 1 cm optical path length) at the CdS band edge absorption peak when diluted by a factor of 100.

Synthesis of Spherical CdS. The synthesis of wurtzite CdS nanocrystals was carried out in a similar manner to an established method.[56] First, 0.046 mg of CdCl$_2$, 0.79 mL of oleic acid and 10 mL of di-n-octylether in a 50 mL three-neck round-bottom flask were heated to 250 °C under Ar atmosphere. Eight mg of sulfur dissolved in 0.825 mL of oleylamine (2.5 mmol) was swiftly injected to the flask with a syringe. After 10 min, the growth was terminated by cooling to room temperature. The resulting CdS NCs were purified by precipitation using a solvent mixture of chloroform and methanol followed by centrifugation. The supernatant was discarded and the precipitate was redispersed in chloroform for the next step.

Synthesis of Spherical CdSe/CdS Nanocrystal. The synthesis of wurtzite CdSe core was carried out in a similar manner to an established method.[57] First, 0.060 g of CdO, 0.28 g of ODPA and 3 g TOPO in a 50 mL flask were degassed at 150 °C for 30 min under vacuum and then heated to 370 °C under Ar atmosphere. At this point, 1.5 g of TOP was injected into the flask. After the temperature recovered to 370 °C, 0.06 g of Se dissolved in 0.5 mL of TOP was swiftly injected into the flask. After 30 s, the growth was terminated by cooling the reaction mixture to room temperature. The resulting CdSe seeds were purified by precipitation using a solvent mixture of chloroform, methanol and butanol and redispersed in chloroform. The synthesis of CdS shell growth was carried out in a similar manner to an established method.[19] The Cd precursor for CdS growth was prepared by heating a mixture of 0.128 g of CdO and 3.16 mL of oleic acid in 10 mL of ODE to 250 °C. After cooling to room temperature, 0.21 mL of octanethiol was added to Cd oleate/ODE solution and the solution was stirred for 30 min until the solution turned clear. For the CdS shell growth, 3 mL of ODE, 3 mL of oleic acid and 200 nmol of previously prepared CdSe seeds in a 50 mL flask were degassed at 150 °C for 30 min under vacuum and then heated to 310 °C under Ar atmosphere. During heating, the mixture of Cd and S precursors was slowly injected at a rate of 3 mL/h starting at 240 °C. Once the injection was finished, 1 mL of oleic acid was swiftly injected into the flask at 310 °C. After 1 h, the growth was terminated by cooling to room temperature. The resulting CdSe/CdS core/shell NCs were purified by precipitation using a solvent mixture of chloroform and methanol followed by centrifugation. The supernatant was discarded and the precipitate was redispersed in chloroform for the next step.

Etching and Regrowth with Metal Oleates. A mixture of 0.184 g of Zn acetate and various amount of oleic acid (from 0.64 to 3.82 mL) in ODE as indicated were prepared in a 50 mL three-neck round-bottom flask and degassed at 120 °C for 30 min under vacuum. Total volume of the reaction was maintained at 6 mL by adjusting the volume of ODE. The solution was then heated to 250 °C to form Zn oleate. After 1 h, the Zn oleate solution was cooled to 60 °C. A purified solution of CdS NRs, CdS NCs, CdS/CdSe NRHs or CdSe/CdS core/shell NCs was injected into the solution and chloroform was allowed to evaporate for 30 min under vacuum. After heating to 250 °C, etching was carried out at this temperature for the duration as indicated. For experiments examining growth using etched Cd in solution, TOPSe solution containing 20 mg of Se in 1.0 mL of TOP was slowly injected at 250 °C at a rate of 4 mL/h and the reaction mixture was allowed to stir at 250 °C for 5 min prior to cooling to room temperature. For high-temperature annealing, the solution was heated to 300 °C after TOPSe injection and the reaction temperature was maintained at 300 °C for 5 min before being cooled down to room temperature. For Na oleate etching, the procedure was the same as the Zn oleate case except 0.304 g of Na oleate was used instead of Zn acetate and oleic acid. For the control experiment to test the effect of oleic acid, the same procedure was used except that only 1.13 mL of oleic acid was added without Zn acetate or Na oleate.

Characterization. TEM samples were prepared on Au grids with thin carbon film from a dilute solution of NCs in chloroform. TEM analysis was carried out with a JEOL 2100 TEM operating at 200 kV. EDS and STEM analyses were carried out with a JEOL JEM-2200FS aberration-corrected STEM/TEM operating at 200 kV. UV−vis absorption spectra were obtained with an Agilent 8453 photodiode array spectrometer. PL spectra were collected with a Horiba Jobin Yvon FluoroMax-3 spectrofluorometer. The moisture content of reaction mixtures was determined by Karl Fischer titration with Photovolt Aquatest CMA using HYDRANAL reagents.

■ ASSOCIATED CONTENT

Ⓢ Supporting Information

The Supporting Information is available free of charge on the ACS Publications website at DOI: 10.1021/jacs.6b03834.

Additional TEM and STEM images, spectra, and EDS data (PDF)

■ AUTHOR INFORMATION

Corresponding Author

*mshim@illinois.edu

Notes

The authors declare no competing financial interest.

■ REFERENCES

(1) Li, J. J.; Wang, Y. A.; Guo, W.; Keay, J. C.; Mishima, T. D.; Johnson, M. B.; Peng, X. *J. Am. Chem. Soc.* **2003**, *125* (41), 12567.

(2) Peng, X.; Manna, L.; Yang, W.; Wickham, J.; Scher, E.; Kadavanich, A.; Alivisatos, A. *Nature* **2000**, *404* (6773), 59.

(3) Manna, L.; Milliron, D. J.; Meisel, A.; Scher, E. C.; Alivisatos, A. P. *Nat. Mater.* **2003**, *2* (6), 382.

(4) Ithurria, S.; Talapin, D. V. *J. Am. Chem. Soc.* **2012**, *134* (45), 18585.

(5) Kwon, S. G.; Krylova, G.; Phillips, P. J.; Klie, R. F.; Chattopadhyay, S.; Shibata, T.; Bunel, E. E.; Liu, Y.; Prakapenka, V. B.; Lee, B.; Shevchenko, E. V. *Nat. Mater.* **2015**, *14* (2), 215.

(6) Qu, L.; Peng, Z. A.; Peng, X. *Nano Lett.* **2001**, *1* (6), 333.

(7) Bullen, C. R.; Mulvaney, P. *Nano Lett.* **2004**, *4* (12), 2303.

(8) Goebl, J. A.; Black, R. W.; Puthussery, J.; Giblin, J.; Kosel, T. H.; Kuno, M. *J. Am. Chem. Soc.* **2008**, *130* (44), 14822.

(9) Protesescu, L.; Yakunin, S.; Bodnarchuk, M. I.; Krieg, F.; Caputo, R.; Hendon, C. H.; Yang, R. X.; Walsh, A.; Kovalenko, M. V. *Nano Lett.* **2015**, *15* (6), 3692.

(10) Choi, S.-H.; Na, H.; Park, Y.; Il, K.; Kwon, S. G.; Jang, Y.; Park, M.-H.; Moon, J.; Son, J. S.; Song, I. C.; Moon, W. K.; Hyeon, T. *J. Am. Chem. Soc.* **2008**, *130* (46), 15573.

(11) Milliron, D. J.; Hughes, S. M.; Cui, Y.; Manna, L.; Li, J.; Wang, L.-W.; Alivisatos, A. P. *Nature* **2004**, *430* (6996), 190.

(12) García-Rodríguez, R.; Liu, H. *J. Am. Chem. Soc.* **2014**, *136* (5), 1968.

(13) Joo, J.; Na, H.; Yu, T.; Yu, J. H.; Kim, Y. W.; Wu, F.; Zhang, J. Z.; Hyeon, T. *J. Am. Chem. Soc.* **2003**, *125* (36), 11100.

(14) Ma, Y.; Zeng, J.; Li, W.; McKiernan, M.; Xie, Z.; Xia, Y. *Adv. Mater.* **2010**, *22* (17), 1930.

(15) Peng, Z. A.; Peng, X. *J. Am. Chem. Soc.* **2001**, *123* (1), 183.

(16) Hung, L.-I.; Tsung, C.-K.; Huang, W.; Yang, P. *Adv. Mater.* **2010**, *22* (17), 1910.

(17) McDaniel, H.; Oh, N.; Shim, M. *J. Mater. Chem.* **2012**, *22* (23), 11621.

(18) Cozzoli, P. D.; Pellegrino, T.; Manna, L. *Chem. Soc. Rev.* **2006**, *35* (11), 1195.

(19) Chen, O.; Zhao, J.; Chauhan, V. P.; Cui, J.; Wong, C.; Harris, D. K.; Wei, H.; Han, H.-S.; Fukumura, D.; Jain, R. K.; Bawendi, M. G. *Nat. Mater.* **2013**, *12* (5), 445.

(20) Acharya, K. P.; Nguyen, H. M.; Paulite, M.; Piryatinski, A.; Zhang, J.; Casson, J. L.; Xu, H.; Htoon, H.; Hollingsworth, J. A. *J. Am. Chem. Soc.* **2015**, *137* (11), 3755.

(21) Han, M.; Gao, X.; Su, J. Z.; Nie, S. *Nat. Biotechnol.* **2001**, *19* (7), 631.

(22) Wegner, K. D.; Hildebrandt, N. *Chem. Soc. Rev.* **2015**, *44* (14), 4792.

(23) Zhan, N.; Palui, G.; Mattoussi, H. *Nat. Protoc.* **2015**, *10* (6), 859.

(24) McDaniel, H.; Pelton, M.; Oh, N.; Shim, M. *J. Phys. Chem. Lett.* **2012**, *3* (8), 1094.

(25) Lee, S.; Flanagan, J. C.; Kang, J.; Kim, J.; Shim, M.; Park, B. *Sci. Rep.* **2015**, *5*, 17472.

(26) Shim, M.; Mcdaniel, H.; Oh, N. *J. Phys. Chem. Lett.* **2011**, *2* (21), 2722.

(27) Bang, J.; Park, J.; Lee, J. H.; Won, N.; Nam, J.; Lim, J.; Chang, B. Y.; Lee, H. J.; Chon, B.; Shin, J.; Park, J. B.; Choi, J. H.; Cho, K.; Park, S. M.; Joo, T.; Kim, S. *Chem. Mater.* **2010**, *22* (1), 233.

(28) Chen, Y.; Vela, J.; Htoon, H.; Casson, J. L.; Werder, D. J.; Bussian, D. A.; Klimov, V. I.; Hollingsworth, J. A. *J. Am. Chem. Soc.* **2008**, *130* (15), 5026.

(29) Han, X.; Zhou, X.; Jiang, Y.; Xie, Z. *J. Mater. Chem.* **2012**, *22* (21), 10924.

(30) Hofmann, C.; Rusakova, I.; Ould-Ely, T.; Prieto-Centurión, D.; Hartman, K. B.; Kelly, A. T.; Lüttge, A.; Whitmire, K. H. *Adv. Funct. Mater.* **2008**, *18* (11), 1661.

(31) Yu, W. W.; Peng, X. *Angew. Chem., Int. Ed.* **2002**, *41* (13), 2368.

(32) Park, J.; An, K.; Hwang, Y.; Park, J.-G.; Noh, H.-J.; Kim, J.-Y.; Park, J.-H.; Hwang, N.-M.; Hyeon, T. *Nat. Mater.* **2004**, *3* (12), 891.

(33) Li, R.; Lee, J.; Yang, B.; Horspool, D. N.; Aindow, M.; Papadimitrakopoulos, F. *J. Am. Chem. Soc.* **2005**, *127* (8), 2524.

(34) Oh, N.; Kim, J. H.; Jin, S.; Yoon, C. S. *Small* **2009**, *5* (11), 1311.

(35) Lee, D.; Kim, W. D.; Lee, S.; Bae, W. K.; Lee, S.; Lee, D. C. *Chem. Mater.* **2015**, *27* (15), 5295.

(36) Battaglia, D.; Blackman, B.; Peng, X. *J. Am. Chem. Soc.* **2005**, *127* (31), 10889.

(37) Khon, E.; Lambright, K.; Khnayzer, R. S.; Moroz, P.; Perera, D.; Butaeva, E.; Lambright, S.; Castellano, F. N.; Zamkov, M. *Nano Lett.* **2013**, *13* (5), 2016.

(38) Xiong, Y.; Chen, J.; Wiley, B.; Xia, Y.; Aloni, S.; Yin, Y. *J. Am. Chem. Soc.* **2005**, *127* (20), 7332.

(39) Li, R.; Luo, Z.; Papadimitrakopoulos, F. *J. Am. Chem. Soc.* **2006**, *128* (19), 6280.

(40) Lim, S. J.; Kim, W.; Shin, S. K. *J. Am. Chem. Soc.* **2012**, *134* (18), 7576.

(41) Lim, S. J.; Kim, W.; Jung, S.; Seo, J.; Shin, S. K. *Chem. Mater.* **2011**, *23* (22), 5029.

(42) Torimoto, T.; Reyes, J. P.; Iwasaki, K.; Pal, B.; Shibayama, T.; Sugawara, K.; Takahashi, H.; Ohtani, B. *J. Am. Chem. Soc.* **2003**, *125* (2), 316.

(43) Mulvihill, M. J.; Ling, X. Y.; Henzie, J.; Yang, P. *J. Am. Chem. Soc.* **2010**, *132* (1), 268.

(44) Ryu, E.; Kim, S.; Jang, E.; Jun, S.; Jang, H.; Kim, B.; Kim, S.-W. *Chem. Mater.* **2009**, *21* (4), 573.

(45) Liu, D.; Xu, X.; Du, Y.; Qin, X.; Zhang, Y.; Ma, C.; Wen, S.; Ren, W.; Goldys, E. M.; Piper, J. A.; Dou, S.; Liu, X.; Jin, D. *Nat. Commun.* **2016**, *7*, 10254.

(46) Hotje, U.; Rose, C.; Binnewies, M. *Solid State Sci.* **2003**, *5* (9), 1259.

(47) Advincula, R. C. *Dalt. Trans.* **2006**, *58* (23), 2778.

(48) Katari, J. E. B.; Colvin, V. L.; Alivisatos, A. P. *J. Phys. Chem.* **1994**, *98* (15), 4109.

(49) Li, Z.; Ji, Y.; Xie, R.; Grisham, S. Y.; Peng, X. *J. Am. Chem. Soc.* **2011**, *133* (43), 17248.

(50) García-Rodríguez, R.; Hendricks, M. P.; Cossairt, B. M.; Liu, H.; Owen, J. S. *Chem. Mater.* **2013**, *25* (8), 1233.

(51) Müller, A.; Diemann, E. *Adv. Inorg. Chem.* **1987**, *31*, 89.

(52) Cirillo, M.; Aubert, T.; Gomes, R.; Van Deun, R.; Emplit, P.; Biermann, A.; Lange, H.; Thomsen, C.; Brainis, E.; Hens, Z. *Chem. Mater.* **2014**, *26* (2), 1154.

(53) Abe, S.; Capek, R. K.; De Geyter, B.; Hens, Z. *ACS Nano* **2013**, *7* (2), 943.

(54) Oh, N.; Nam, S.; Zhai, Y.; Deshpande, K.; Trefonas, P.; Shim, M. *Nat. Commun.* **2014**, *5*, 3642.

(55) Nam, S.; Oh, N.; Zhai, Y.; Shim, M. *ACS Nano* **2015**, *9* (1), 878.

(56) Saruyama, M.; So, Y.-G.; Kimoto, K.; Taguchi, S.; Kanemitsu, Y.; Teranishi, T. *J. Am. Chem. Soc.* **2011**, *133* (44), 17598.

(57) Carbone, L.; Nobile, C.; De Giorgi, M.; Sala, F.; Morello, G.; Pompa, P.; Hytch, M.; Snoeck, E.; Fiore, A.; Franchini, I. R.; Nadasan, M.; Silvestre, A. F.; Chiodo, L.; Kudera, S.; Cingolani, R.; Krahne, R.; Manna, L. *Nano Lett.* **2007**, *7* (10), 2942.